Journal of Sound and Vibration (2001) **246**(5), 777–793
doi:10.1006/jsvi.2000.3611, available online at http://www.idealibrary.com on IDEAL®

WAVELET ANALYSIS OF VIBRATION SIGNALS OF AN OVERHANG ROTOR WITH A PROPAGATING TRANSVERSE CRACK

S. A. ADEWUSI

Mechanical Engineering Department, King Fahd University of Petroleum and Minerals, P.O. Box 1069, *Dhahran* 31261, *Saudi Arabia. E-mail: sadewusi@kfupm.edu.sa*

AND

B. O. AL-BEDOOR

Mechanical Engineering Department, King Fahd University of Petroleum and Minerals, P.O. Box 841, *Dhahran* 31261, *Saudi Arabia, E-mail: bobedoor@kfupm.edu.sa*

(*Received* 28 *June* 2000, *and in final form* 1 *November* 2000)

This paper presents an experimental study of the dynamic response of an overhang rotor with a propagating transverse crack using the discrete wavelet transform (DWT)—a joint time frequency analysis technique. Start-up and steady state vibration signatures are analyzed using Daubechies (Db6) mother wavelet and the results are presented in the form of scalograms and space-scale energy distribution graphs. The start-up results showed that crack reduces the critical speed of the rotor system. The steady state results showed that propagating crack produces changes in vibration amplitudes of frequency scale levels corresponding to $1X$, $2X$ and $4X$ harmonics. The vibration amplitude of frequency scale level corresponding to $1X$ may increase or decrease depending on the location of the crack and side load. However, the amplitude of frequency scale level corresponding to $2X$ increases continuously as the crack propagates.

1. INTRODUCTION

Overhang rotors are found in many industrial applications. Although rotors are carefully designed for fatigue loading and high level of safety by using high-quality materials and precise manufacturing techniques, catastrophic failures of rotors as a result of cracks can occur particularly in high-speed rotating machines, in which the rotor is carrying discs, blades, gears, etc. of considerable weight, which may induce fatigue crack propagation. Despite the extensive studies of the vibration analysis of cracked rotating shafts for diagnostic purposes, the problem is still not fully understood and no unique identification technique is found.

Due to the importance of detecting cracks in rotors, research was directed towards the use of vibration signals as they provide a non-intrusive detection technique. Many researchers [1–16] modelled and studied the dynamic response of cracked rotors using different approaches. The conventional fast Fourier transform (FFT)-based spectral analysis method was used to analyze steady state vibration signals of cracked rotors. Imam *et al.* [4] used a three-dimensional (3-D) finite element method and a non-linear rotor

0022-460X/01/400777 + 17 $35.00/0

dynamics model to study cracked rotor system vibration and developed an on-line rotor crack detection and monitoring system. Histogram signature analysis, which is the FFT of the difference between the averaged vibration signals from a cracked and an uncracked shaft was used. Experimental results showed $1X$ and $2X$ vibration frequency harmonics. Dirr and Schmalhorst [6] used a vibration measurement method and a potential difference method of fatigue crack measurement to study the shape of cracks at different depth during crack propagation in a rotating shaft. The FFT of experimental vibration signals showed $1X$ and $2X$ harmonics. A three-dimensional (3-D) finite element crack model was also used to study the bending stress distribution near the crack tip. Wauer [9] carried out a comprehensive literature survey of the state-of-the art of the dynamics of cracked rotors. None of the 162 papers cited in reference [9] used wavelet analysis to study vibrations of cracked rotors. Collins *et al.* [11] studied a cracked Timoshenko rotor by solving the six-coupled equations obtained by Wauer [9]. The frequency spectrum of the rotor response to a periodic axial impulse was also studied. The results showed an increase in the coupling between axial, torsional and transverse vibration. Diana *et al.* [12] studied theoretically and experimentally on-line crack detection for turbo-generator rotors with a transverse crack. The difference between the current vibration and the previous vibration is used to calculate the vibration forces. The FFT of vibration signals showed $1X$ and $2X$ harmonic components. Dimarogonas and Papadopoulas [13] studied the stability of cracked rotors in the coupled vibration mode. The frequency spectra of the vibration signal of a 300 MW steam turbine showed high $2X$, $\frac{1}{2}X$ and $\frac{1}{4}X$ vibration components that suggested the existence of deep crack. Wu and Huang [15] studied the dynamic response of a rotor with a transverse crack by numerically solving the dynamic equations of a cracked rotor model. FFT of the response at various speeds, crack depths and crack locations showed $1X$ and $2X$ harmonics. Zheng [16] studied numerically the vibration of a rotor system with a switching crack. He suggested the use of features other than $1X$ and $2X$ harmonics and signal analysis technique other than FFT-based spectral analysis for crack detection. He used Gabor's analysis on the vibration signals after the $1X$ and $2X$ harmonics were removed. His results showed the presence of transient signals.

Other papers reveal that attention was focused on the study of simply supported cracked rotors, the use of FFT-based spectral analysis and orbits in the vibration signals analysis of rotors with transverse crack. It is known that FFT is highly localized only in the frequency domain and that it cannot handle transient or non-stationary signals. The limitation of the FFT led to the development of the joint time frequency analysis technique, of which wavelet transform is a family, giving information in both time and frequency domains. A propagating crack will change continuously the dynamic properties of rotors and the resulting vibration signals. Therefore, wavelet analysis, a joint time frequency analysis technique, will represent the variations in features of vibration signals with time. Spectral analysis gives an averaged result without giving information on time localization. Wavelet transform (WT) is increasingly becoming useful in vibration signals analysis. Some of its unique characteristics are that it can handle both stationary and non-stationary signals, and can transform any signal directly into time/space and frequency/scale domains, which can provide detailed information about signal evolution. Mallat [17], Newland [18] and Burrus *et al.* [19] discussed the theory of wavelets and their applications in signal analysis. Newland [20, 21] presented wavelet transform and wavelet maps in vibration analysis. Onsay and Haddow [22] used wavelet transform to analyze experimental vibration data of the transient flexural vibrations of an impact excited uniform beam. The results showed the efficacy of WT in detecting transient waves in a dispersive medium. Kishimoto *et al.* [23] used WT to analyze dispersive waves in a beam. The results showed that wavelet could decompose strain response into time and frequency components. Hamdan *et al.* [24] carried

out the comparison of various basic wavelets for the analysis of flow-induced vibration of a cylinder in a cross-flow. Newland [25] demonstrated the application of harmonic wavelets in time–frequency mapping of transient signals. The advantage of WT over short-time Fourier transform and Wigner–Ville frequency decomposition methods is that its bandwidth can be chosen arbitrarily and hence it offers a variable Q transform. Aretakis and Mathioudakis [26] applied wavelet analysis to gas turbine fault diagnosis and compared the results with Fourier analysis.

This work presents an experimental study on the dynamic response of an overhang rotor with a propagating transverse crack using the discrete wavelet transform (DWT), a joint time frequency analysis technique. Start-up and steady state vibration signatures are analyzed using Daubechies (DbN) mother wavelet and the results are presented in the form of 2-D and 3-D graphs. The results are presented and discussed and some conclusions are extracted.

2. EXPERIMENTAL SET-UP

The equipment used for the experiment include a rotor kit, rotor kit motor speed control, Data Acquisition Interface Unit (DAIU-208P) with accessories, oscilloscopes, personal computer (PC), eddy current displacement/proximity probes, automated diagnostics for rotating equipment (ADRE) for Windows Software and shafts. The experiment is set-up as shown in Figure 1(a). The proximity probes are connected via auxiliary components to

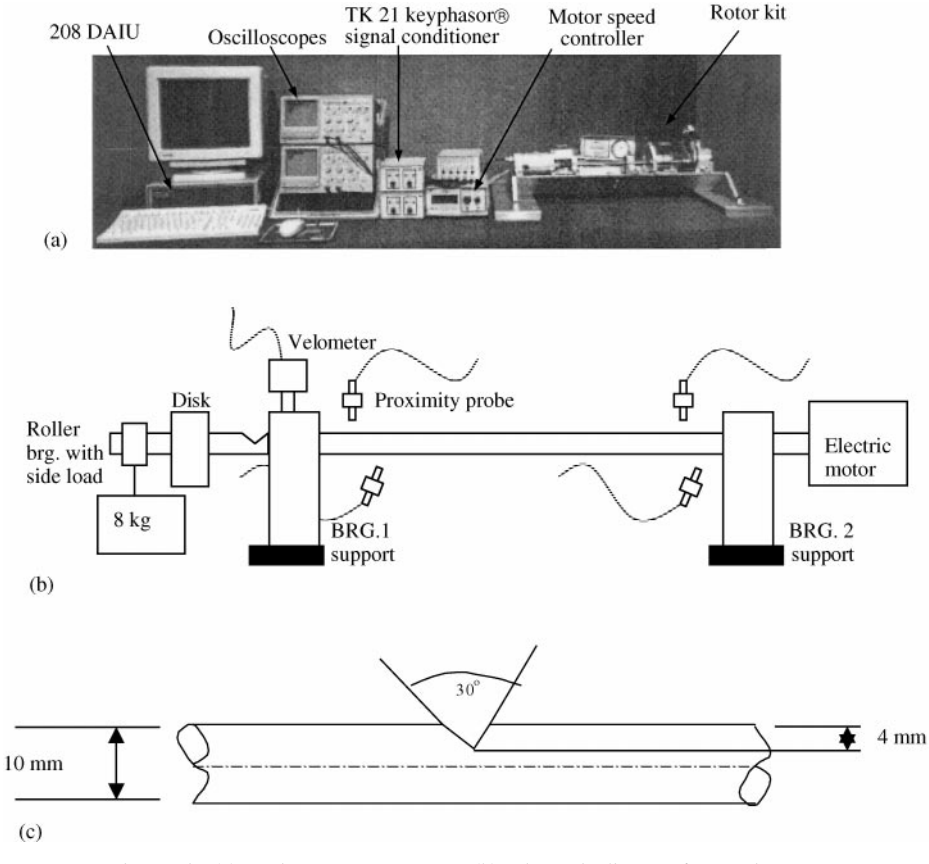

Figure 1. Experiment rig. (a) Equipment arrangement. (b) Schematic diagram for overhang rotor arrangement. (c) Crack geometry.

oscilloscopes to observe the amplitude–time waveforms and orbits of the vibration signals. The probes are connected to the DAIU-208P, which is in turn connected to the PC. The DAIU operation is controlled by the ADRE for Window Software to collect and store vibration data. The vibration signatures are processed using the Daubachies (DbN) wavelet transform.

Figure 1(b) is the schematic diagram of the overhang cracked rotor arrangement. The shaft material is ductile steel bar AISI 4140. The shaft has the following dimensions and material properties: 10 mm diameter, 540 mm length, mass per unit length of 0·72 kg/m, Young's modulus of about 200 GPa. Two discs each of mass 0·8 kg and a hanging side load are fitted on the shaft as shown in Figure 1(b). The hanging side load was applied to aid crack propagation. The shafts are supported in self-lubricating sleeve bearings. Three shafts were machined: one without crack and the other two with 4 mm deep v-notch to induce stress concentration to start propagating the crack. The crack angle is 30° and the crack tip open displacement (CTOD) was measured with the optical microscope and was found to be 0·117 mm. Figure 1(c) shows the crack geometry.

Three experiments were carried out. The first experiment was for the uncracked shaft with the discs and 8 kg hanging side load located at 7 and 13 cm from the bearing support number 1 (Figure 1(b)) respectively. The second experiment consisted of the first cracked shaft with 4 mm depth v-notch surface crack located at 1·5 cm from the bearing support number 1, Figure 1(b). The locations of the discs, 8 kg hanging side load, and bearing supports are the same as those for the first experiment for the uncracked shaft. The third experiment was for the second cracked shaft with 4 mm deep v-notch surface crack located at 3·5 cm from the bearing support number 1. The discs and 8 kg hanging side load are located at 10 and 16 cm from the bearing support number 1 respectively.

The start-up and steady state vibration signals for each experiment are collected and analyzed with the Daubechies wavelet and the results are presented and discussed in the following section. The vibration signals in both the vertical and horizontal directions measured by the proximity probes located close to bearing support number 1 are considered. The steady state running speed for all experiments was 3500 r.p.m., which is higher than the first critical speed of the rotor system.

3. RESULTS AND DISCUSSIONS

Unlike FFT, which gives frequency information directly, wavelet transform (WT) does not give frequency information directly. WT gives a dimensionless scale, which can be related to frequency and dimensionless space, which can be related to time. For this reason, attention and discussion of results will focus on comparison, rather than absolute values, of different features of wavelet graphs; namely the 2-D and 3-D plots. Dyadic discrete wavelet transform (DWT) using Daubechies mother wavelet (Db6) in MATLAB Wavelet Toolbox [27] is used for the analyses. The relationship between frequency f and wavelet scale a is $f \propto 1/a$. For the dyadic discrete wavelet transform, Scale a is defined as $a = 2^j$, where $j = 1, 2, 3 \ldots$ is the frequency level. Each level represents a unique frequency resolution. The dyadic scale a increases in multiples of 2, e.g., the lowest frequency resolution scale is 2 followed by 4, 8, 16, etc.

Wavelet analysis of start-up and steady state vibration signals are presented in the form of 2-D and 3-D graphs. Since dyadic scale a is defined as 2^j, changes in critical speed of the rotor system that are not multiples of 2 cannot be clearly identified along the scale-axis (y-axis) of the 2-D graphs of start-up signals. Therefore, small changes in critical speed can be identified on the start-up 2-D graphs (scalograms) by considering the time or position of

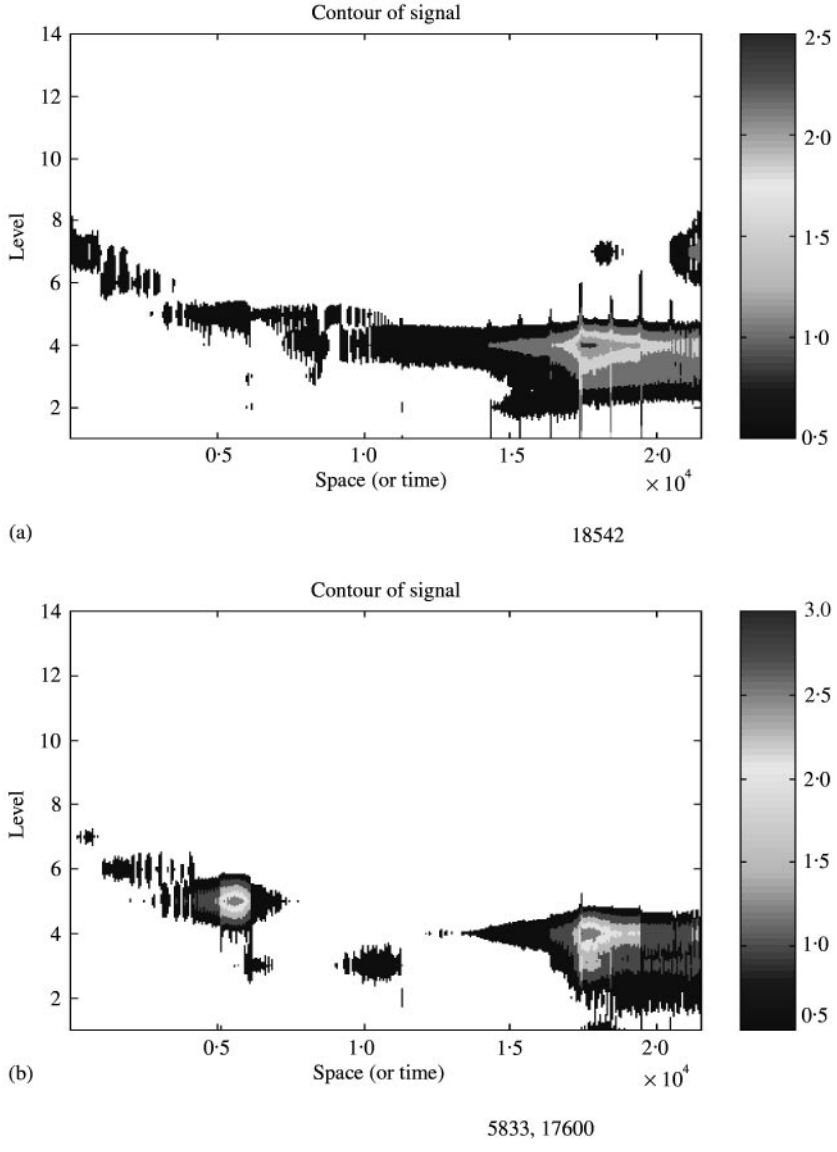

Figure 2. Scalogram of start-up signal for uncracked shaft with 8 kg hanging side load. (a) Vertical. (b) Horizontal.

resonance along the space (or dimensionless time) axis. During start-up, the rotor speed increases with time, which is represented as space on wavelet 2-D graphs; hence the position of the resonance is proportional to the critical speed. The centre point of the position of resonance for each start-up scalogram is indicated below in each graph.

The steady state vibration response of any system usually contains harmonics and sub-harmonics of the excitation frequency. Therefore, $1X$, $2X$, $4X$ and $8X$ vibration harmonics can easily be identified on steady state wavelet scalograms with the highest scale level corresponding to $1X$. The vertical overhang 8 kg side load was attached to the rotor (Figure 1(b)) to induce stress on the v-notch to aid crack propagation.

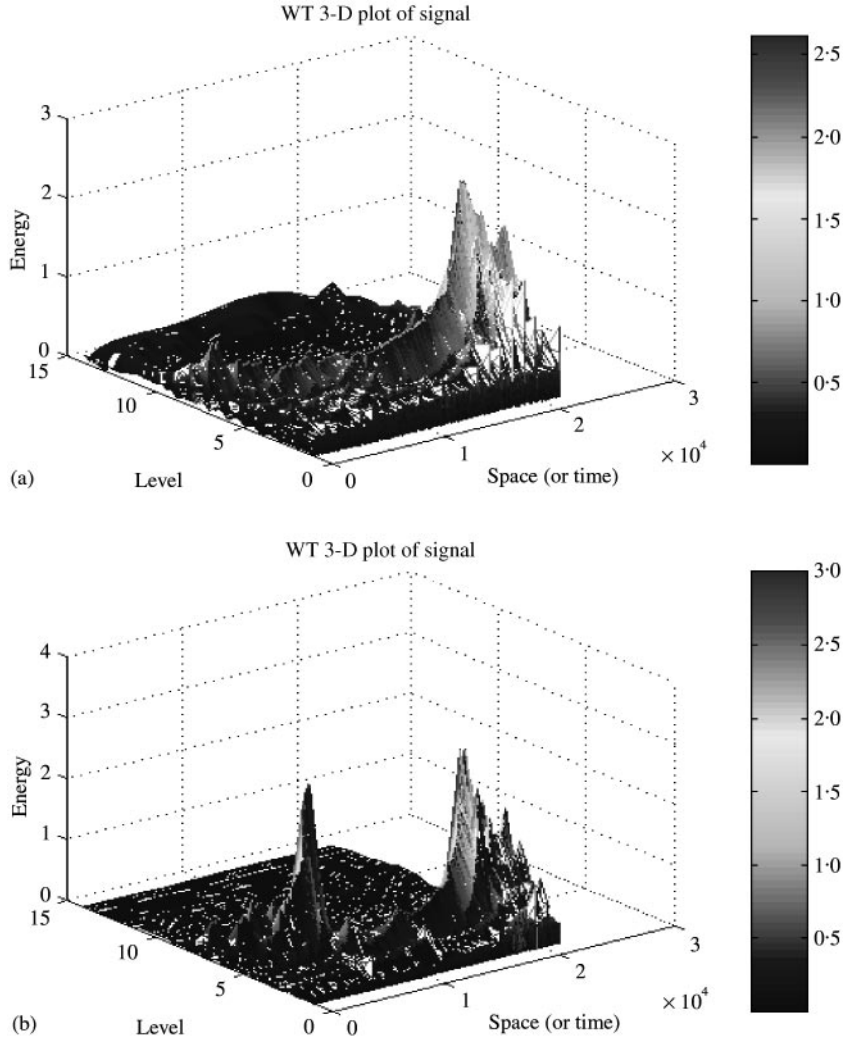

Figure 3. 3-D plot of start-up signals for uncracked shaft with 8 kg hanging side load. (a) Vertical. (b) Horizontal.

In the scalogram (the 2-D plot), the x- and y-axis represent dimensionless time and frequency levels respectively. The intensity indicates the vibration amplitude as shown by the intensity scale. The 3-D plots show dimensionless time and frequency level on the plane, the energy axis indicates the vibration amplitude.

3.1. UNCRACKED SHAFT

Figures 2 and 3 represent the 2-D (scalogram) and the 3-D plot of start-up signals for the uncracked shaft. Resonance occurred at frequency level 4 and position 18542 in the vertical direction with wide resonance bandwidth (Figure 2(a)). In the horizontal direction, it occurred at level 5, position 5833 and level 4, position 17600 (Figure 2(b)). The regions without any trace in Figure 2(b) correspond to the vibration region with amplitude less than

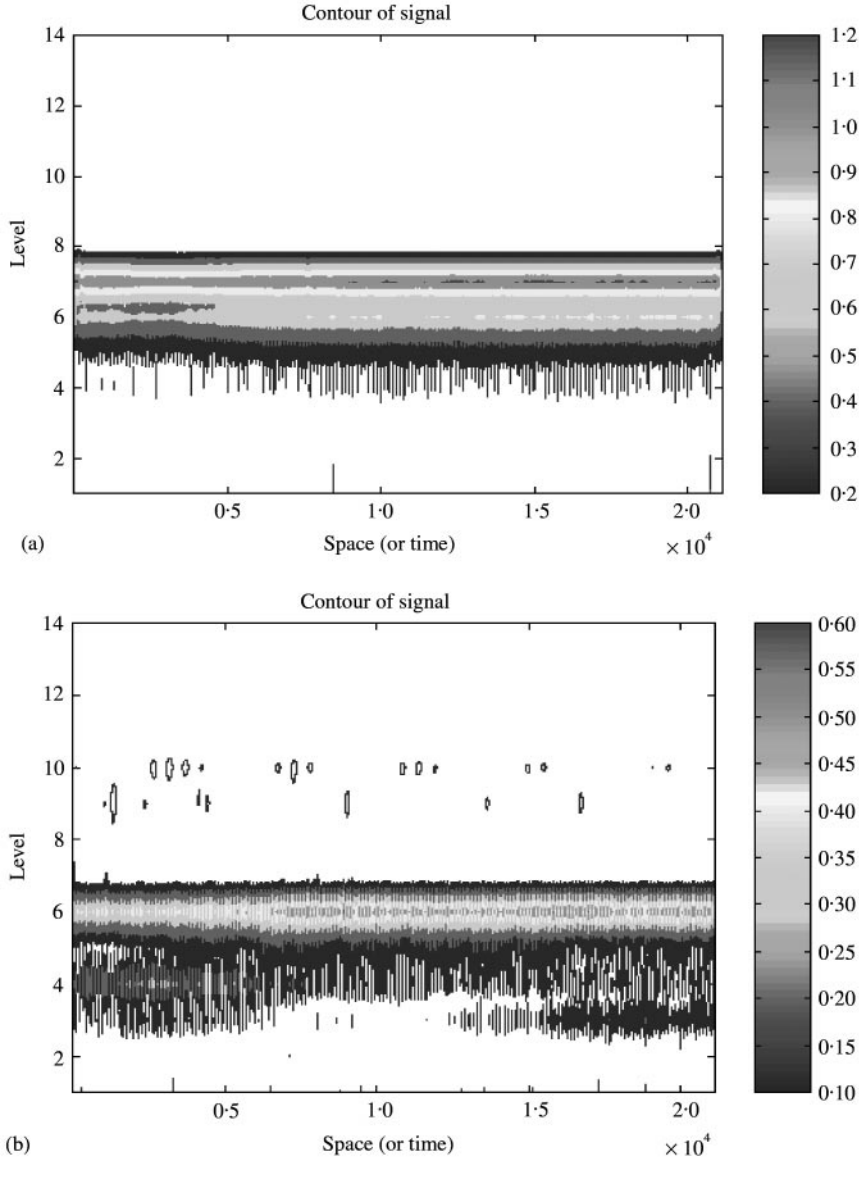

Figure 4. Scalogram of steady state signals for uncracked shaft with 8 kg hanging side load. (a) Vertical. (b) Horizontal.

0·5 mil. The contour plot that is used to get the scalograms chooses the intensity range by default neglecting small amplitude values compared with the maximum value. In the 3-D plot, (Figure 3) the minimum amplitude is zero, therefore all amplitudes are well represented.

Figures 4 and 5 present the wavelet analysis results for the steady state vibration of the uncracked shaft with an 8 kg hanging load and at a speed of 3500 r.p.m. Two prominent frequency levels, levels 7 and 6 corresponding to $1X$ and $2X$ harmonics, respectively, are present in Figure 4(a) and 5(a). The vibration amplitude at level 7 ($1X$) is higher than that at level 6 ($2X$). In Figures 4(b) and 5(b), only level 6 is prominent. Since this is the highest level,

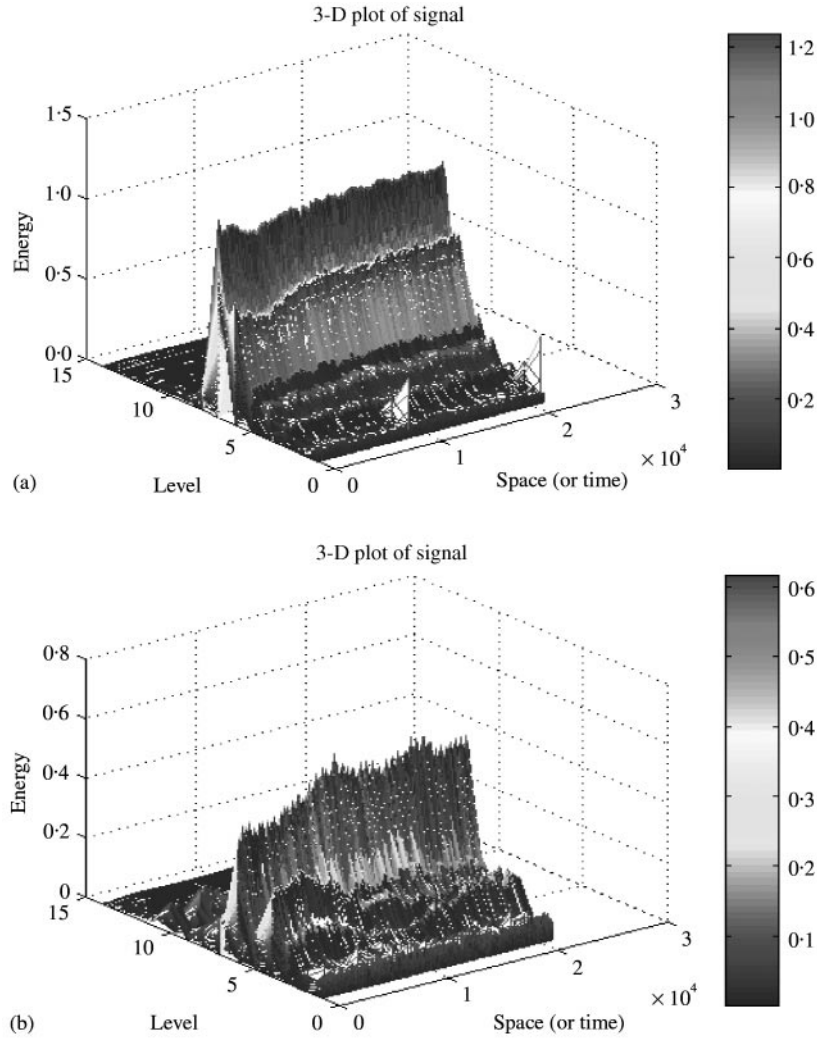

Figure 5. 3-D plot of steady state signals for uncracked shaft with 8 kg hanging side load. (a) Vertical. (b) Horizontal.

it corresponds to $1X$ vibration. The amplitude of vibration in the horizontal direction (Figure 5(b)) is unsteady. Also, some scattered spots appeared between levels 8 and 10 in Figure 4(b). These features in the horizontal direction suggest the presence of transient vibration, which may be due to non-linearity in the system and the gyroscopic effect of the overhang masses.

3.2. CRACKED SHAFT

Scalograms and 3-D graphs of start-up signals for the first cracked shaft are presented in Figures 6 and 7. The resonance position in the vertical direction (Figure 6(a)) occurred at 15417 with a bandwidth smaller than the bandwidth in Figure 3(a). The resonance positions in the horizontal direction (Figure 6(b)) occurred at 4167 and 15100 for the first and second

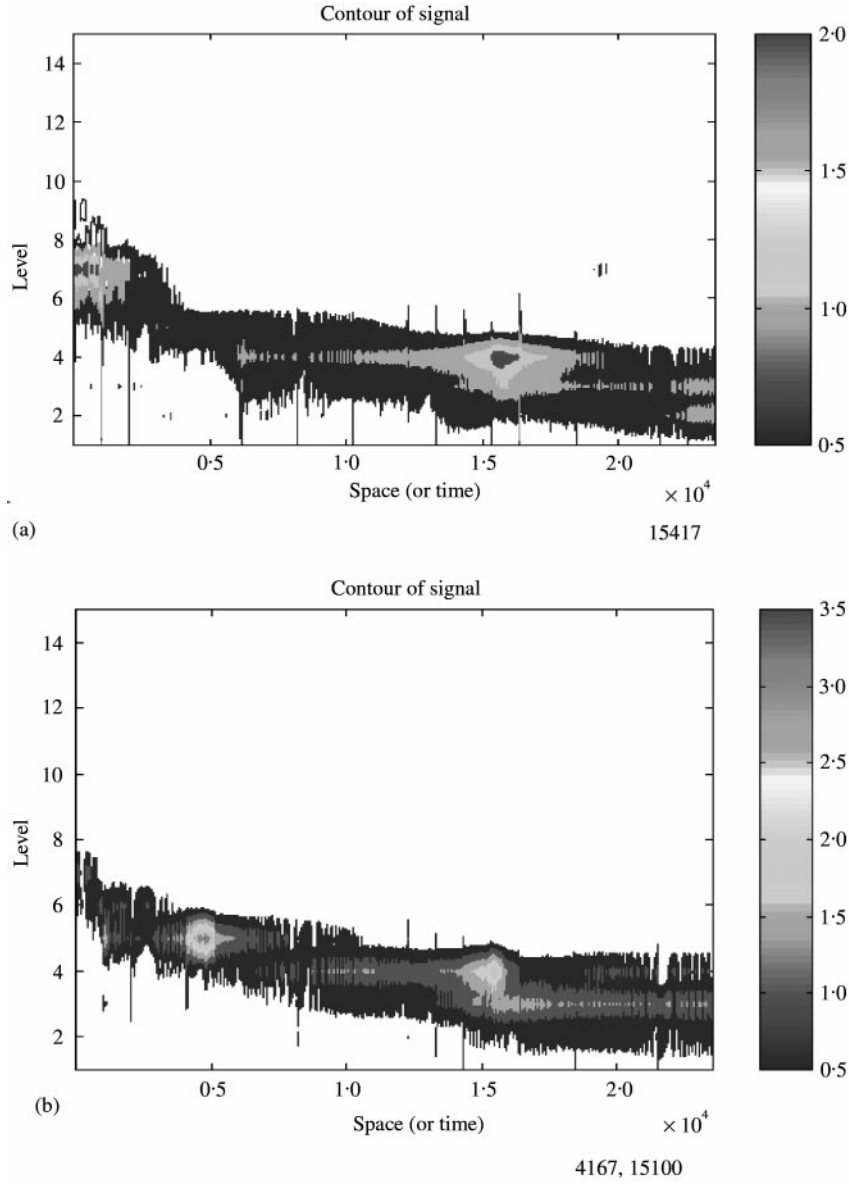

Figure 6. Scalogram of start-up signals for the first shaft with 4 mm notch crack and 8 kg hanging side load. (a) Vertical. (b) Horizontal.

critical speeds respectively. The resonance bandwidths in the horizontal direction are also smaller than the bandwidths for the uncracked shaft, Figure 3(b). Comparison of Figures 6 and 7 for the first cracked shaft and Figures 3 and 4 for the uncracked shaft show that the crack decreases the critical speed in both directions, as shown by the positions of resonance. The results are consistent with the results of Dimaroganas and Paipetis [3]; they reported that a crack reduces the stiffness of shaft, which is reflected in the decrease in critical speed. The start-up experiment for the first cracked shaft was repeated three times, which caused crack propagation and the shaft fractured after few minutes when rotated at a steady state

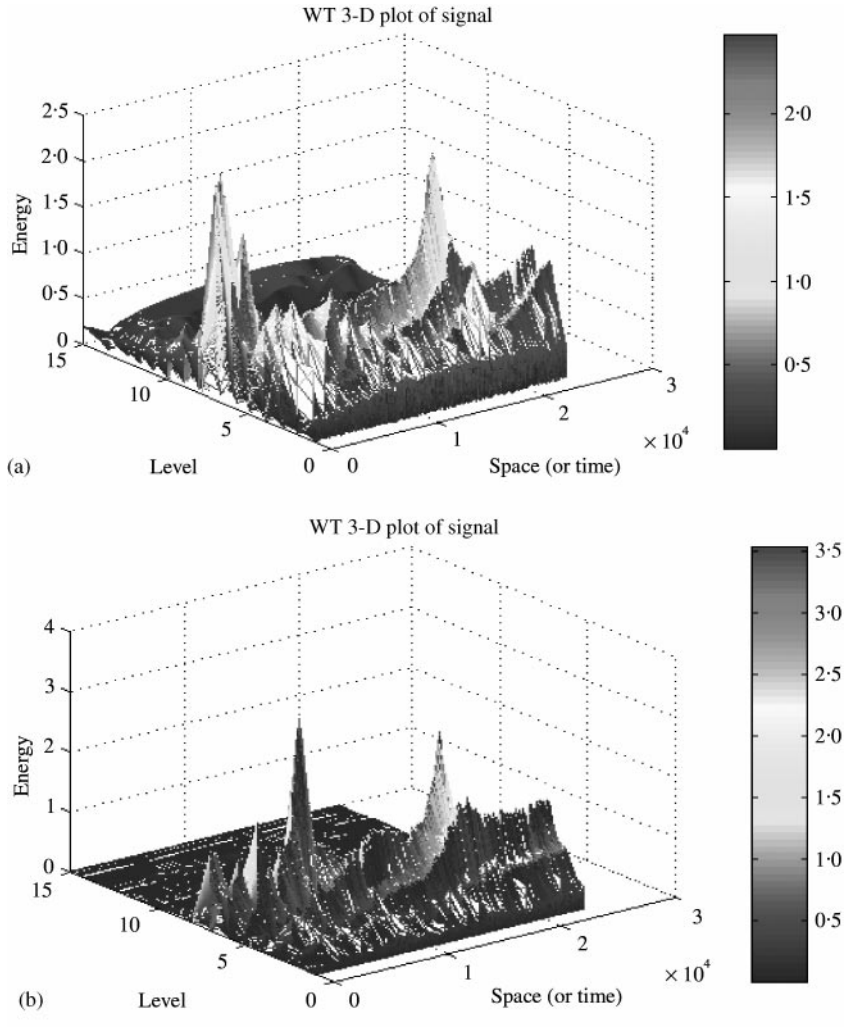

Figure 7. 3-D plot of start-up signals for the first shaft with 4 mm notch crack and 8 kg hanging side load. (a) Vertical. (b) Horizontal.

speed of 3500 r.p.m. as shown in Figures 8 and 9. Figures 8 and 9 show scalograms and 3-D graphs of steady state signals for the first cracked shaft. Two levels (6 and 5) corresponding to $1X$ and $2X$ harmonics, respectively, are present. Figures 8 and 9 show that crack propagation produces a tremendous increase in the vibration amplitude of level 5 ($2X$ harmonic), far greater than level 6 ($1X$) until the shaft fractured. This observation agrees with the results reported by Gasch [1], Grabowski [2], Imam *et al.* [4], Inagaki *et al.* [5]. Dirr and Shmalhorst [6], Davies and Mayes [7] and Diana *et al.* [12]. After the fracture of the rotor, level 5 ($2X$) amplitude became very small compared with level 6 ($1X$) amplitude.

Figures 10 and 11 represent the scalogram and the 3-D plot of start-up signals for the second cracked shaft experiment. Resonance occurred at level 4 and point 15625 in the vertical direction with a small resonance bandwidth (Figure 10(a)) while it occurred at level 5, position 4670 and level 4, position 15330 in the horizontal direction (Figure 10(b)). The

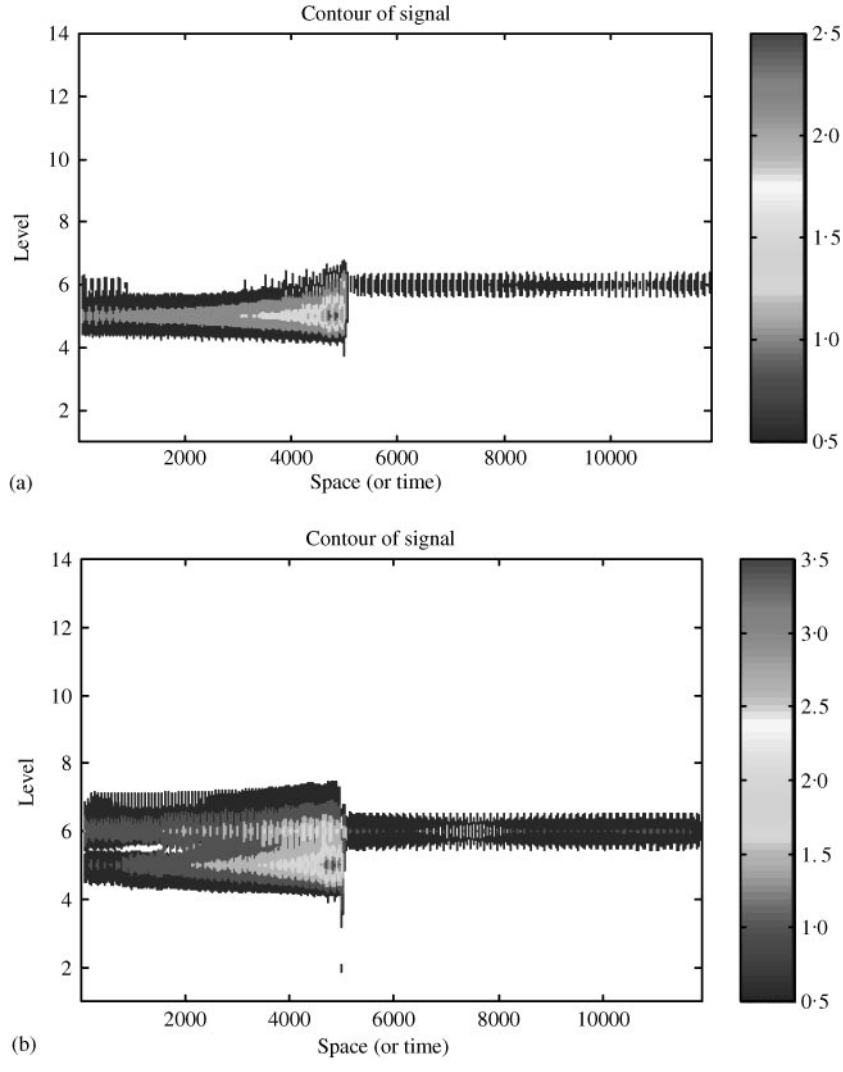

Figure 8. Scalogram of the steady state signals for first shaft with 4 mm notch crack and 8 kg hanging side load. (a) Vertical. (b) Horizontal.

results for the uncracked and the two cracked shafts show that the influence of a crack on the stiffness and dynamic response of a rotor system depends on the crack location. Gasch [1] and Meng and Hahn [14] reported the same observation. Figures 12 and 13 show steady state results for the second cracked shaft. The results show that vibration amplitudes of levels 6 and 5 corresponding to $2X$ and $4X$ harmonics increase continuously as the crack propagates; the increase in $2X$ amplitude is, however, higher than $4X$ amplitude. The change in amplitude of level 7 ($1X$) is small compared with levels 6 and 5 corresponding to $2X$ and $4X$ harmonics respectively. The wavelet transformation was used in the monitoring of the vibration of cracked rotors. The results of this study, particularly for the steady state response of the cracked shaft, have very clearly captured the propagation of the crack in the rotating shaft in the form of exponential increase in $2X$ vibration amplitudes in 3-D plots.

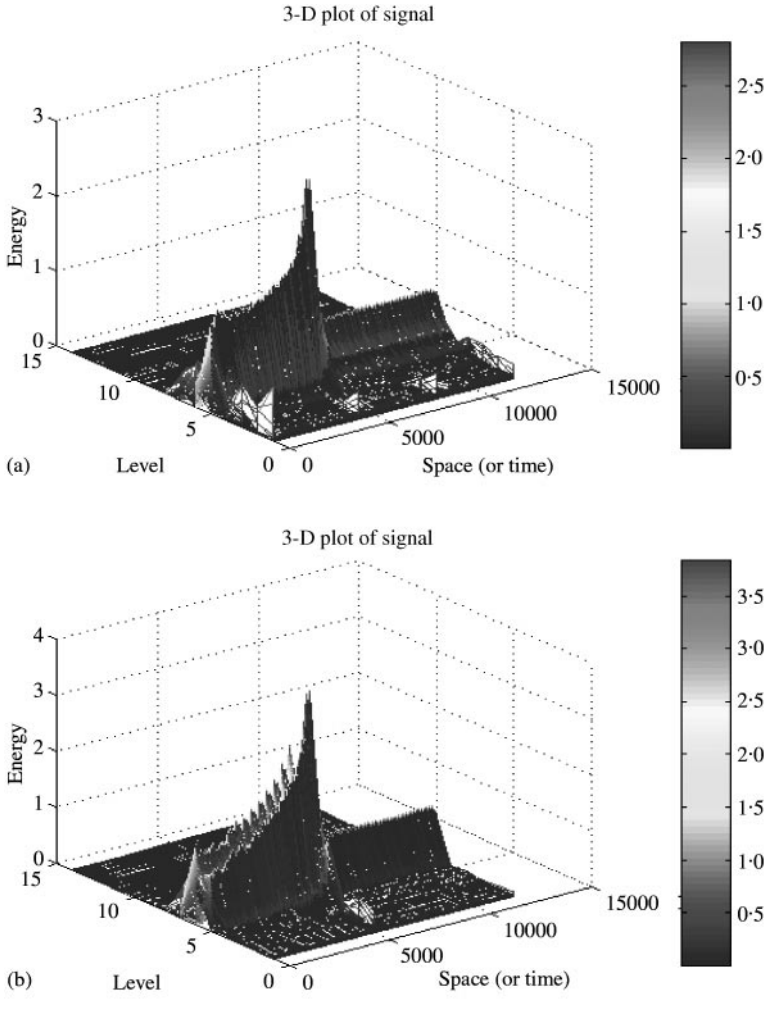

Figure 9. 3-D plot of the steady state signals for the first shaft with 4 mm notch crack and 8 kg hanging side load. (a) Vertical. (b) Horizontal.

The rate at which this component ($2X$) grows can be an excellent way of detecting propagating cracks.

4. CONCLUSIONS

Wavelet analysis of vibration signals of an overhang rotor with a 4 mm v-notch propagating transverse crack is presented. The dyadic discrete wavelet transform using Daubechies (Db6) mother wavelet of start-up and steady-state vibration signals for uncracked and cracked rotors are presented in the form of 2-D graphs known as scalograms and 3-D graphs called space-scale energy distribution graphs. Wavelet transform, a joint time frequency analysis technique, gave a good pictorial representation of the changing features in vibration signals of a rotor with a propagating crack. The start-up results

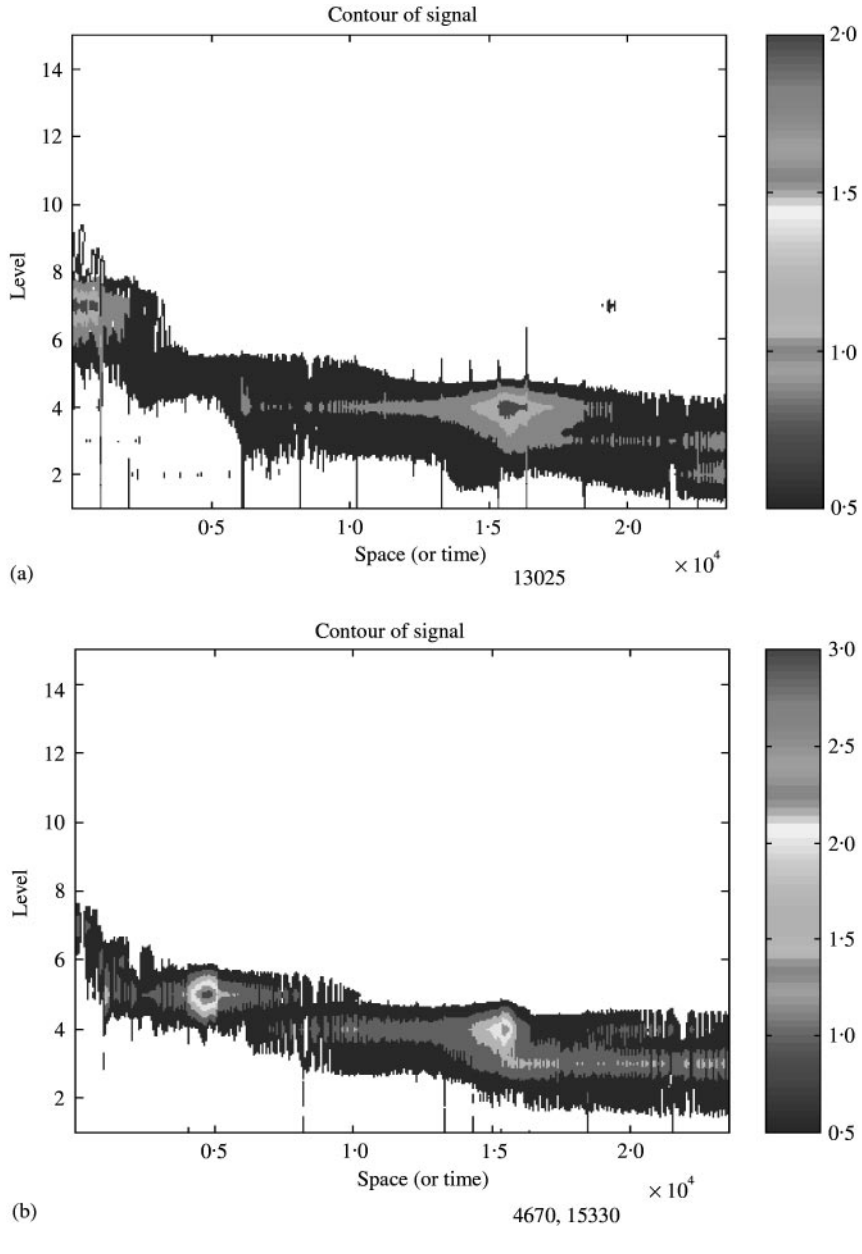

Figure 10. Scalogram of start-up signals for the second shaft with 4 mm notch crack and 8 kg hanging side load. (a) Vertical. (b) Horizontal.

showed that the crack reduces the critical speed of the rotor system. The steady state results showed that the propagating crack produces continuous changes in vibration amplitudes of frequency scale levels corresponding to $1X$, $2X$ and $4X$. During crack propagation, the vibration amplitude of the frequency scale level corresponding to $1X$ may increase or decrease depending on the location of the crack, while the amplitude of the frequency scale corresponding to $2X$ always increases continuously as the crack propagates; this can

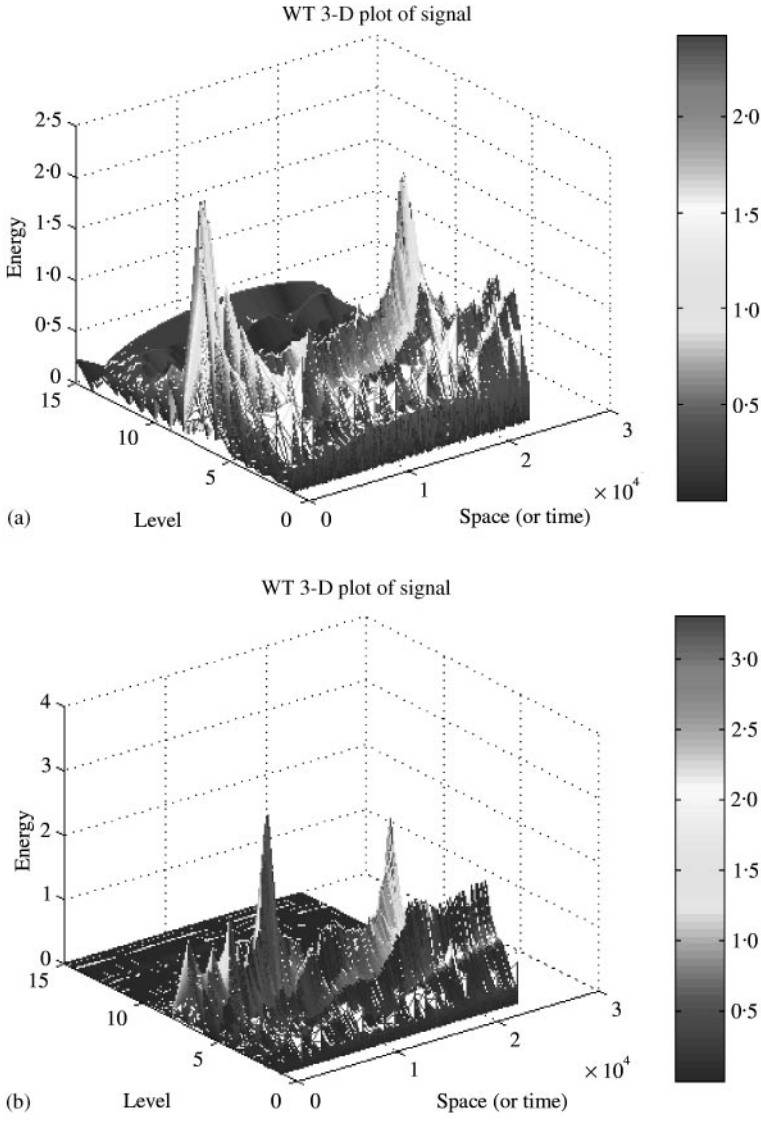

Figure 11. 3-D plot of start-up signals for the second shaft with 4 mm notch crack and 8 kg hanging side load. (a) Vertical. (b) Horizontal.

provide an excellent tool for predicting the existence of a propagating crack. Changes in amplitudes of $1X$ and $2X$ vibration harmonics at a constant running speed are an important feature that distinguishes a propagating crack from imbalance and misalignment, which usually show constant amplitude. Wavelet analysis presents these relative changes in amplitude very clearly; this feature is not present in other signal-processing techniques that are not localized in time and frequency. Further studies using mathematical modelling to quantify the rate of change in $2X$ vibration amplitude and how this can be related to the changing crack depth are recommended.

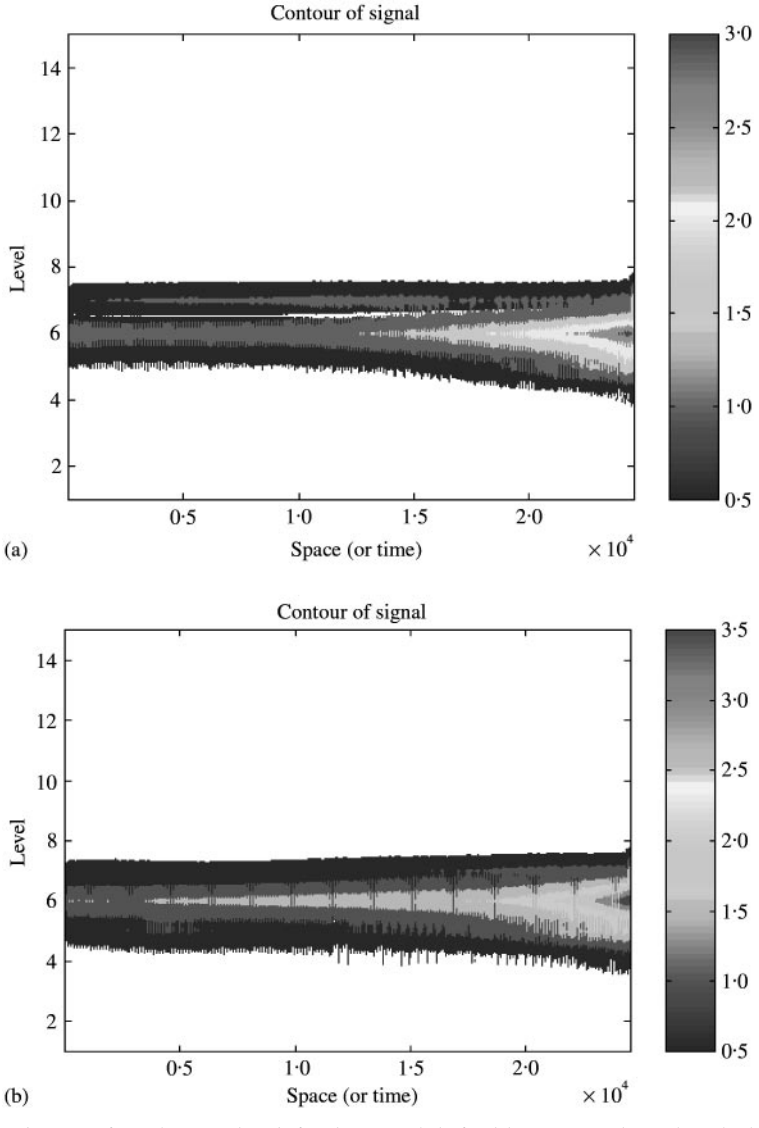

Figure 12. Scalogram of steady state signals for the second shaft with 4 mm notch crack and 8 kg hanging side load. (a) Vertical. (b) Horizontal.

ACKNOWLEDGMENTS

The authors acknowledge the support of King Fahd University of Petroleum and Minerals, Dhahran, Saudi Arabia. The support of Mr. Don Bently of Bently Nevada Corporation, Minden-Nevada, U.S.A. is also acknowledged and appreciated.

REFERENCES

1. R. GASCH 1993 *Journal of Sound and Vibration* **160**, 313–332. A survey of the dynamic behavior of a simple rotating shaft with a transverse crack.

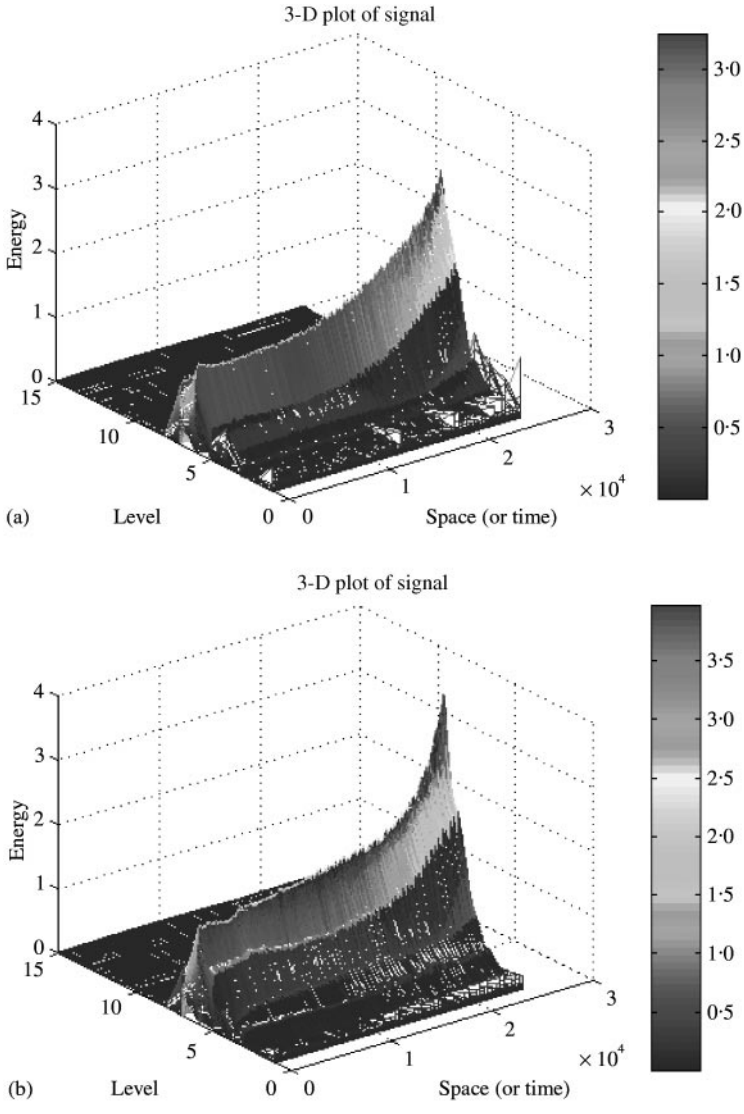

Figure 13. 3-D plot of steady state signals for the second shaft with 4 mm notch crack and 8 kg hanging side load. (a) Vertical. (b) Horizontal.

2. B. GRABOWSKI 1980 *Transactions of the American Society of Mechanical Engineers* **102**, 141–146. The vibrational behavior of a turbine rotor containing a transverse crack.
3. A. D. DIMAROGONAS and S. PAIPETIS 1983 *Analytical Methods in Rotor Dynamics*. London: Applied Science Publishers.
4. S. H. IMAM, R. J. AZZARO BANKERT and J. SCHEIBEL 1989 *Journal of Vibration Acoustics Stress and Reliability in Design* **111**, 241–250. Development of an on-line rotor crack detection and monitoring system.
5. T. INAGAKI, H. KANKI and S. SHIRAKI 1982 *Journal of Mechanical Design* **104**, 345–355. Transverse vibrations of a general cracked rotor bearing system.
6. B. O. DIRR and B. K. SCHMALHORST 1987 11th *ASME Conference on Mechanical Vibration and Noise*, *Boston*, 607–614. Crack depth analysis of a rotating shaft by vibration measurements.

7. I. W. MAYES and W. G. R. DAVIES 1984 *Journal of Vibration Acoustics Stress and Reliability in Design* **106**, 139–145. Analysis of the response of a multi-rotor-bearing system containing a transverse crack in a rotor.
8. D. E. BENTLY and R. F. BOSMANS 1989 *Orbit*. **10**, 8–12. Case study of shaft crack failure.
9. J. WAUER 1990 *Applied Mechanics Review* **43**, 13–17. On the dynamics of cracked rotors: a literature survey.
10. J. WAUER 1990 *International Journal of Solids Structures* **26**, 901–914. Modeling and formulation of equations of motion for cracked rotating shafts.
11. K. R. COLLINS and R. H. PLAUT, E. VIA and J. WAUER 1991 *Transactions of the American Society of Mechanical Engineers* **113**, 74–78. Detection of cracks in rotating Timoshenko shafts using axial impulses.
12. G. DIANA, N. BACHSCHMID and F. ANGELI 1986 *Proceedings of International Conference on Rotordynamics, Tokyo*, 385–390. An on-line crack detection method for turbogenerator rotors.
13. A. D. DAMAROGONAS and C. A. PAPADOPOULAS 1983 *Journal of Sound and Vibration* **91**, 583–593. Vibration of cracked shaft in bending.
14. G. MENG and E. J. HAHN 1997 *Journal of Engineering for Gas Turbine* **119**, 447–455. Dynamic response of a cracked rotor with some comments on crack detection.
15. M-C. WU and S.-S. HUANG 1998 *Journal of Vibration and Acoustics* **120**, 551–555. In-plane vibration and crack detection of a rotating shaft-disk containing a transverse crack.
16. G. T. ZHENG 1998 *Journal of Engineering for Gas Turbine* **120**, 149–154. Vibration of a rotor system with a switching crack and detection of the crack.
17. S. G. MALLAT 1989 *IEEE Transactions on Pattern Analysis and Machine Intelligence* **11**, 674–693. A theory for multiresolution signal decomposition: the wavelet representation.
18. D. E. NEWLAND 1993 *An Introduction to Random Vibrations Spectral and Wavelet Analysis*. Singapore: Longman: third edition.
19. C. BURRUS, A. SIDNEY RAMESH and H. GUO 1998 *Introduction to Wavelets and Wavelet Transforms*: *A primer*. NJ, U.S.A.: Prentice-Hall PTR.
20. D. E. NEWLAND 1994 *Journal of Vibration and Acoustics* **116**, 409–416. Wavelet analysis of vibration, Part 1: Theory.
21. D. E. NEWLAND 1994 *Journal of Vibration and Acoustics* **116**, 417–425. Wavelet analysis of vibration. Part 2: Wavelet Maps.
22. T. ONSAY and A. G. HADDOW 1994 *Journal of the Acoustical Society of America* **95**, 1441–1449. Wavelet transform analysis of transient wave propagation in a dispersive medium.
23. K. KISHIMOTO, H. INOUE, M. HAMADA and T. SHIBUYA 1995 *Journal of Applied Mechanics* **62**, 841–846. Time-frequency analysis of dispersive waves by means of wavelet transform.
24. M. N. HAMDAN, B. A. JUBRAN, N. H. SHABANEH and M. ABU-SAMAK 1996 *Journal of Fluids and Structures* **10**, 1–19. Comparison of various basic wavelets for the analysis of flow induced vibration of a cylinder in cross flow.
25. D. E. NEWLAND. 1997 *Fifth International Congress on Sound and Vibration*. Application of harmonic wavelets to time-frequency mapping. Adelaide, South Australia.
26. N. ARETAKIS and K. MATHIOUDAKIS 1997 *Transaction of the American Society of Mechanical Engineers* **119**, 870–876. Wavelet analysis for gas turbine fault diagnostics.
27. M. MISITI, Y. MISITI, G. OPPENHEIM and J.-M. POGGI 1996 *Wavelet Toolbox for Use with MATLAB*: the Mathworks Inc. MA, U.S.A.